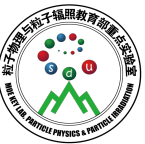


Exploring the QCD Phase Diagram for a Signature of the Critical Point

Jian Deng 邓建 (Shandong University)

with: Jiunn-Wei Chen, Hiroaki Hohenyama, Lance Labun
arXiv: [1410.5454\(PRD\)](#), [1509.04968\(PRD\)](#), [1603.05198](#)

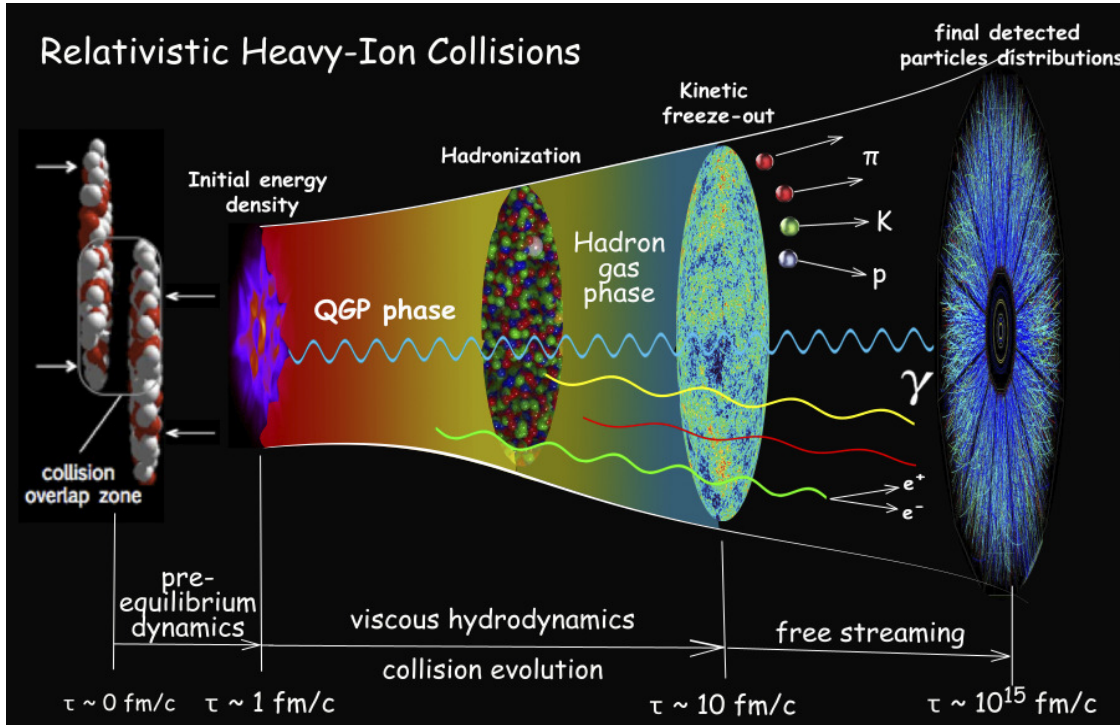
[QCD Phase Structure III, CCNU June 6-9, 2016](#)



Outlines

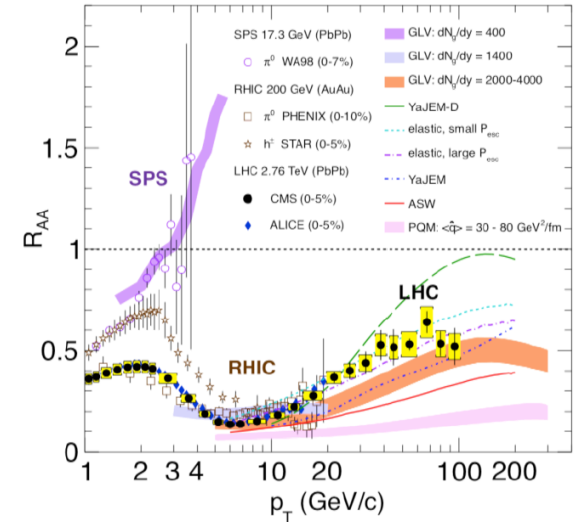
1. Motivation (from QCD to QGP)
2. Phase diagram and CP (from CP to BES)
3. A signature of the criticality
4. Observables: calculation vs. Data
5. Summary

QGP with Little Bang



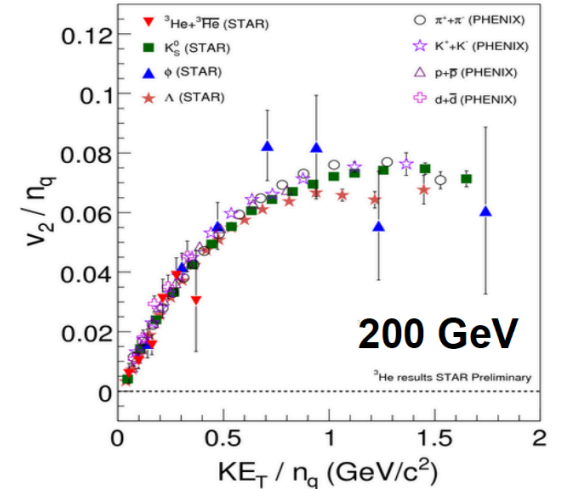
- QGP and phase diagram studied in heavy ion collisions since 1987 at AGS(5GeV), 1996 at SPS(17GeV), since 2000 at RHIC (200GeV), since 2010 at LHC(2.76TeV).
- **Indirect** evidence for strongly coupled and liquid like QGP formed in HIC.
- Trying to search for the **direct pictures** about phase transition. **Strong and special !**

Jet Quenching

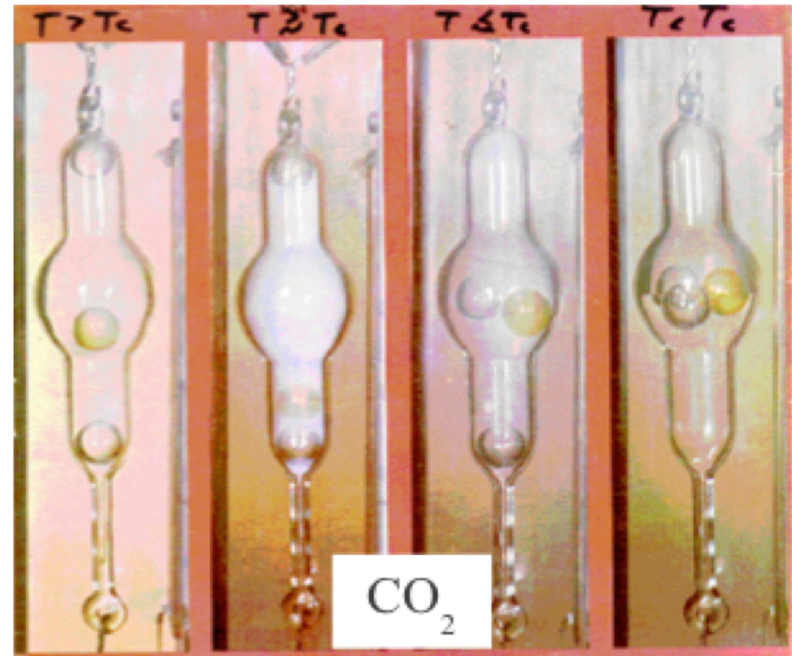
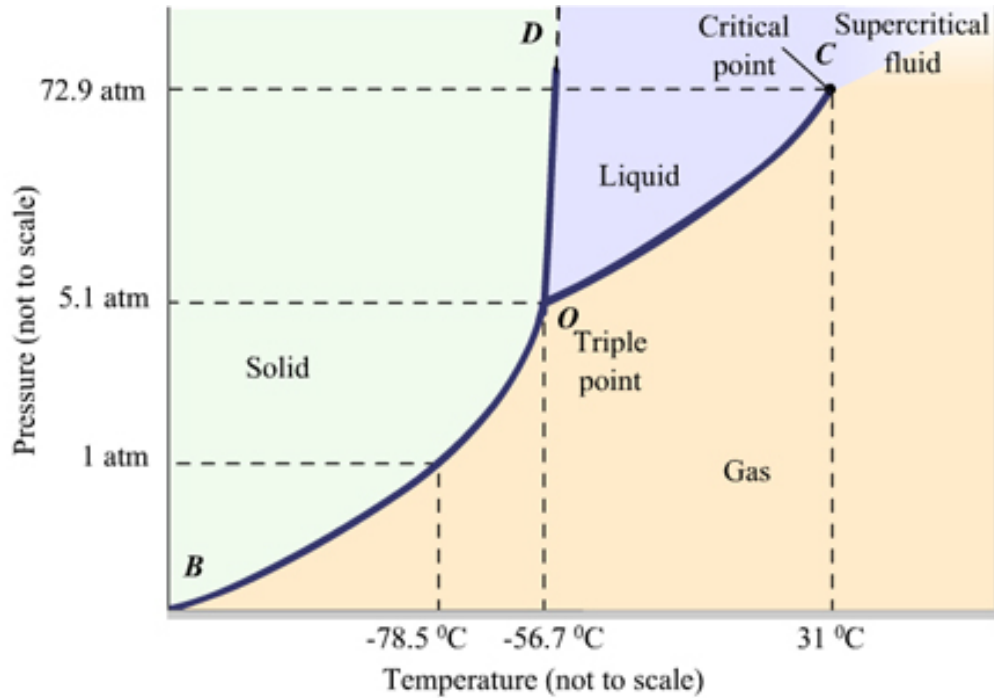


Eur.Phys.J. C72, 1945 (2012).

Partonic Collectivity v_2



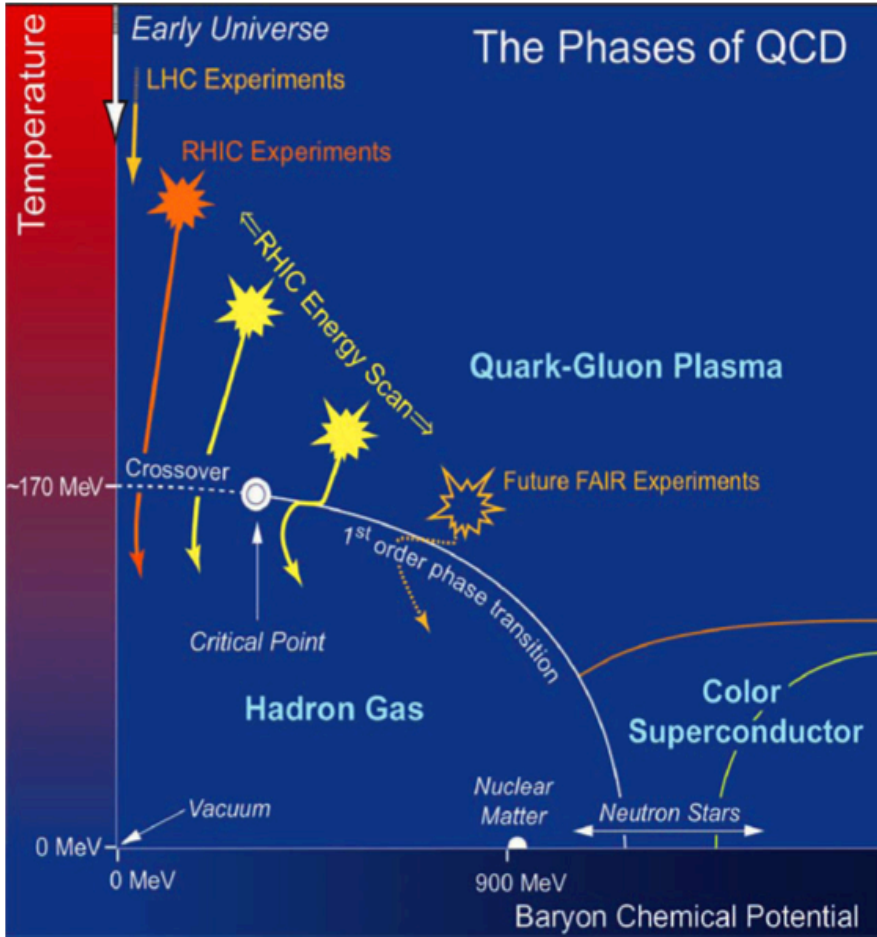
Critical Point and Critical Opalescence



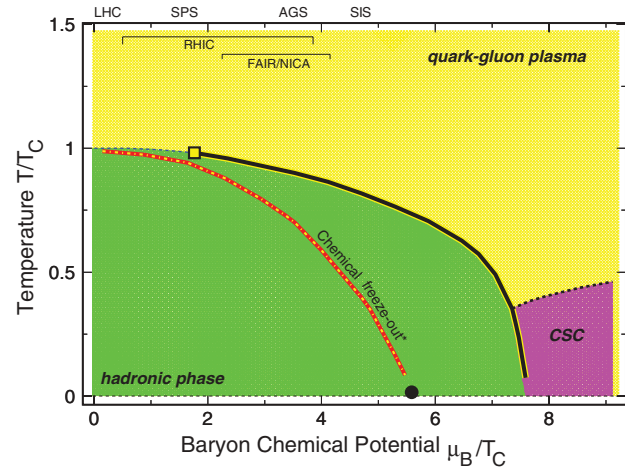
Critical point: End of a first order phase transition line + crossover

Critical opalescence: As the CP approached, the density begin to fluctuate over a large length scales, comparable to the wave length of light. (for CO₂ gas, $0.3\text{nm} \rightarrow 600\text{nm}$)

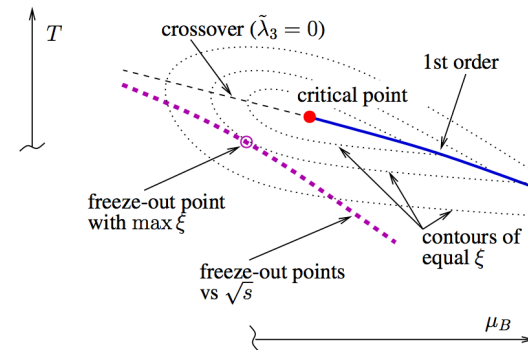
QCD Phase Diagram, Beam Energy Scan



STAR white paper 2014, [Studying the phase diagram of QCD matter at RHIC](#)

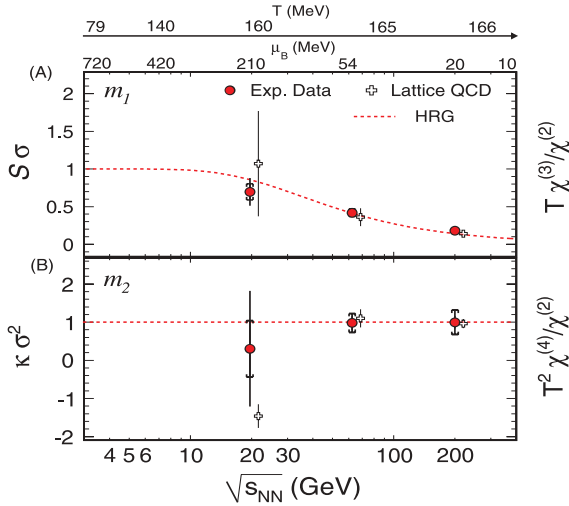


Chemical freeze-out line VS. QCD phase boundary, **mapping**



measurement VS. thermal equilibrium, **singularity**

Lattice and Experimental approaches



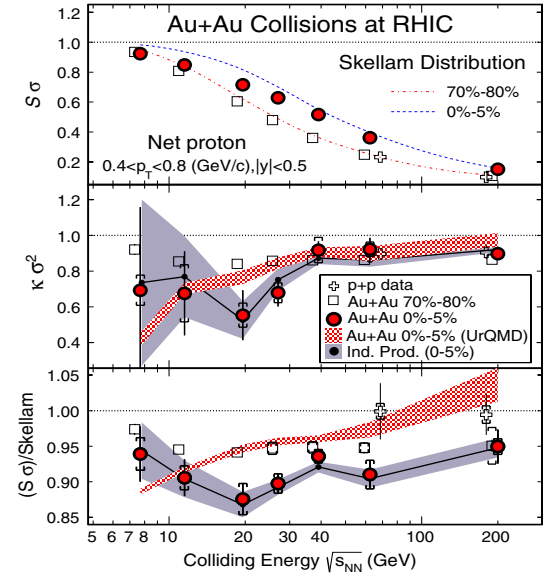
$$T^{n-4} \chi_B^{(n)} \left(\frac{T}{T_c}, \frac{\mu_B}{T} \right) = \frac{1}{T^4} \frac{\partial^n}{\partial (\mu_B/T)^n} P \left(\frac{T}{T_c}, \frac{\mu_B}{T} \right) \Big|_{T/T_c}$$

$$(m_1) : S\sigma = \frac{[B^3]}{[B^2]} = \frac{T \chi_B^{(3)}}{\chi_B^{(2)}}$$

$$(m_2) : \kappa \sigma^2 = \frac{[B^4]}{[B^2]} = \frac{T^2 \chi_B^{(4)}}{\chi_B^{(2)}}$$

$$(m_3) : \frac{\kappa \sigma}{S} = \frac{[B^4]}{[B^3]} = \frac{T \chi_B^{(4)}}{\chi_B^{(3)}}$$

RHIC BES STAR PRL 2014



Scale for the Phase Diagram of QCD

S. Gupta, X. Luo, B. Mohanty, H. G. Ritter, N. Xu, [Science 2011](#)

Sign Problem in Lattice: $\det(D + m + \mu \gamma_0)^* = \det(D + m - \mu^* \gamma_0)$, H-T Ding, et al, [Int. J. Mod. Phys. E 2015](#)

Extrapolate from mu=0: $P(T, \mu) = P(T) + \frac{\mu^2}{2!} \chi^{(2)}(T) + \frac{\mu^4}{4!} \chi^{(4)}(T) + \dots$ C.R.Allton, et al, [PRD 2002](#)

Shoot from imaginary: $\log Z(\mu_I) = a_0 - a_2 \mu_I^2 + a_4 \mu_I^4 + O(\mu_I^6)$. M. Alford, et al, [PRD 2003](#)

Spin imbalanced Fermi gas on a lattice: J. Braun, J-W Chen, JD, et al. [PRL 2013](#)

Higher moments are crucial in HIC

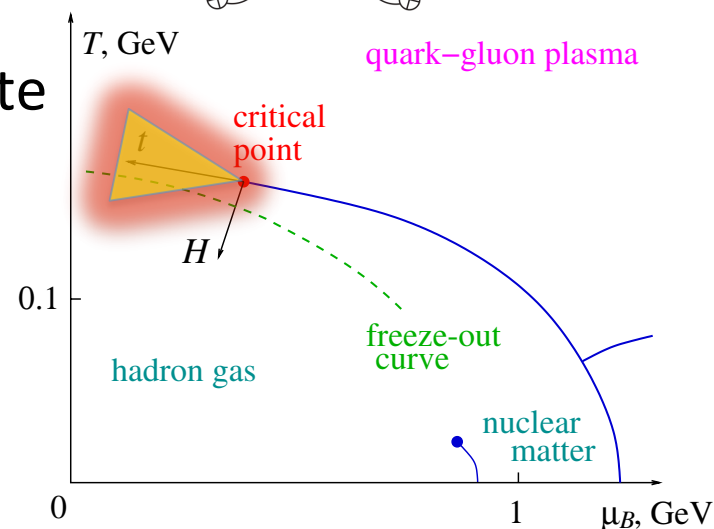
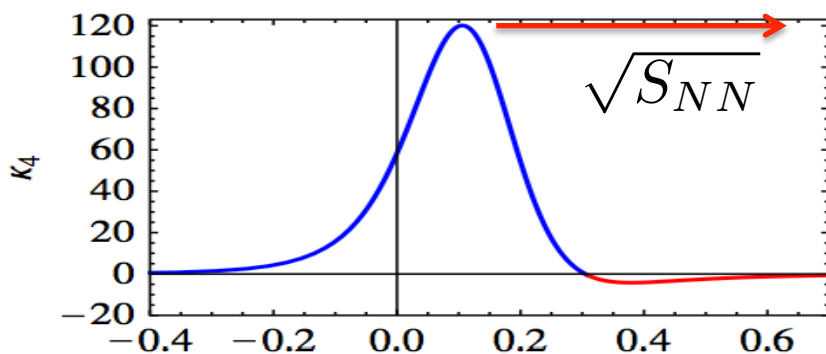
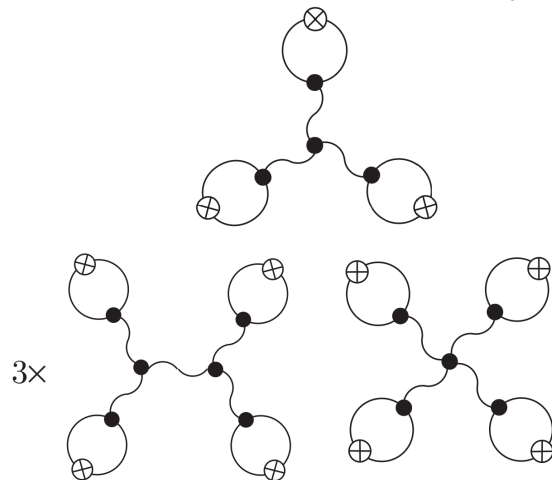
Maximum correlation length 2~3 fm (dynamical evolution, freeze out...)

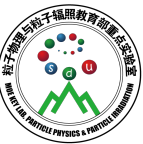
$$\kappa_2 = \langle \sigma_0^2 \rangle = \frac{T}{V} \xi^2; \quad \kappa_3 = \langle \sigma_0^3 \rangle = \frac{2\lambda_3 T}{V} \xi^6;$$

$$\kappa_4 = \langle \sigma_0^4 \rangle_c \equiv \langle \sigma_0^4 \rangle - 3\langle \sigma_0^2 \rangle^2 = \frac{6T}{V} [2(\lambda_3 \xi)^2 - \lambda_4] \xi^8.$$

Non-monotonic functions of the collision energy, higher moments more **sensitive** signature of CP. M. Stephanov, [PRL 2009](#)

Universally, sign change of Kurtosis indicate that CP is close. M. Stephanov, [PRL 2011](#)





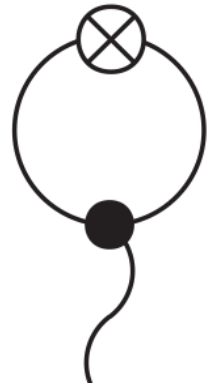
From phase diagram to observables

Susceptibilities = Cumulants

$$\begin{aligned}
 T \frac{\partial}{\partial \mu} \log Z &= \langle N \rangle = \bar{N} \\
 T^2 \frac{\partial^2}{\partial \mu^2} \log Z &= \langle (N - \bar{N})^2 \rangle \\
 T^3 \frac{\partial^3}{\partial \mu^3} \log Z &= \langle (N - \bar{N})^3 \rangle \\
 T^4 \frac{\partial^4}{\partial \mu^4} \log Z &= \langle (N - \bar{N})^4 \rangle - 3 \langle (N - \bar{N})^2 \rangle^2
 \end{aligned}$$

Partition function:

$$Z = \text{Tr} \left[\exp \left(-\frac{H - \mu N}{T} \right) \right]$$

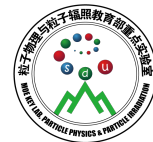


By coupling the critical sigma field with the number density, the fluctuation and the criticality will be transferred to the measurements

M. Stephanov, [PRL 2011](#)

$$\langle (\delta N)^4 \rangle_c = \langle N \rangle + \langle \sigma_V^4 \rangle_c \left(\frac{gd}{T} \int_p \frac{n_p}{\gamma_p} \right)^4 + \dots,$$

Most singular part



Susceptibility

Effective potential: $\Omega(\mu, T, \sigma)$ Grand Canonical ensemble

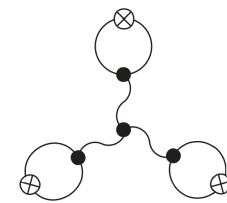
$$\text{Partition function: } Z = \int [d\sigma] \exp\left(-\frac{\Omega(T, \mu, \sigma)}{T}\right)$$

$$T \frac{\partial}{\partial \mu} \log Z = -\left\langle \frac{\partial \Omega[\mu, T, \sigma]}{\partial \mu} \right\rangle = -\langle \Omega' \rangle$$

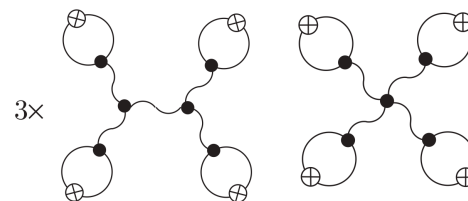
$$T^2 \frac{\partial^2}{\partial \mu^2} \log Z = -T \langle \Omega'' \rangle + \left(\frac{\partial^2 \Omega(\mu, T, \sigma_0)}{\partial \mu \partial \sigma} \right)^2 \langle \delta\sigma^2 \rangle$$

$$T^3 \frac{\partial^3}{\partial \mu^3} \log Z = -T^2 \langle \Omega''' \rangle + \left(\frac{\partial^2 \Omega(\mu, T, \sigma_0)}{\partial \mu \partial \sigma} \right)^3 \langle \delta\sigma^3 \rangle + \dots$$

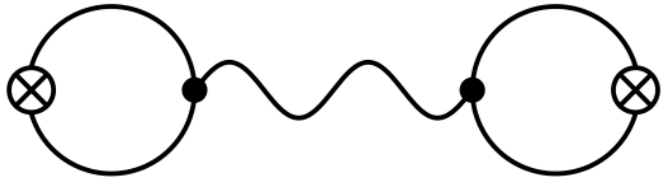
$$T^4 \frac{\partial^4}{\partial \mu^4} \log Z = -T^3 \langle \Omega'''' \rangle + \left(\frac{\partial^2 \Omega(\mu, T, \sigma_0)}{\partial \mu \partial \sigma} \right)^4 (\langle \delta\sigma^4 \rangle - 3\langle \delta\sigma^2 \rangle^2) + \dots$$



Sign change \rightarrow near zeros \rightarrow small
how about other terms?



Tree level contribution

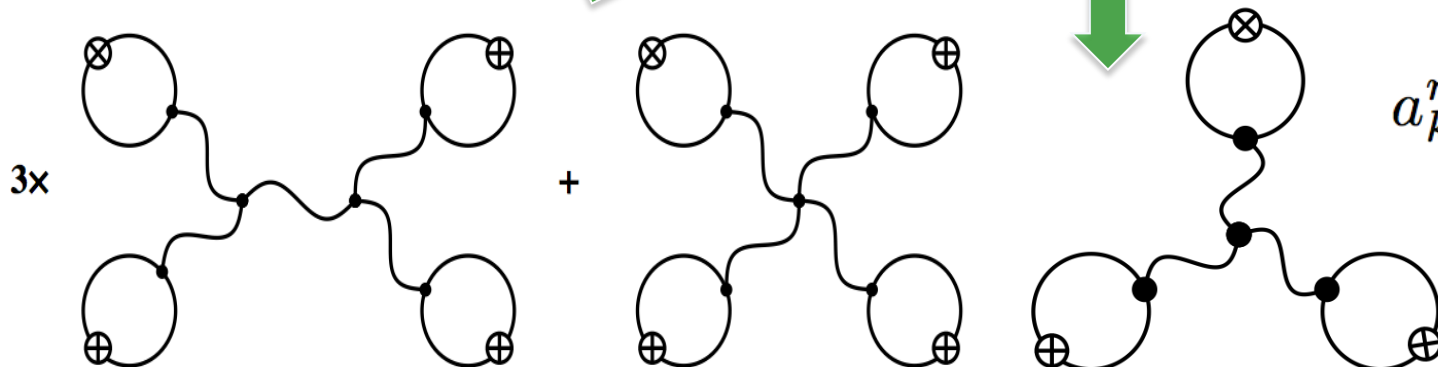
$$T^2 \frac{d^2}{d\mu^2} \log Z = -T a_2^0 + (a_1^1)^2 \langle \delta\sigma^2 \rangle \longrightarrow \text{Diagram 1}$$


$$T^3 \frac{d^3}{d\mu^3} \log Z = -T^2 a_3^0 + 3T a_1^1 a_2^1 \langle \delta\sigma^2 \rangle - (a_1^1)^3 \langle \delta\sigma^3 \rangle - 6(a_1^1)^2 a_2^2 \langle \delta\sigma^2 \rangle^2$$

$$T^4 \frac{d^4}{d\mu^4} \log Z = -T^3 a_4^0 + 3T^2 (a_2^2)^2 \langle \delta\sigma^2 \rangle + 4T^2 a_1^1 a_3^1 \langle \delta\sigma^2 \rangle - 6T (a_1^1)^2 a_2^1 \langle \delta\sigma^3 \rangle$$

$$+ (a_1^1)^4 (\langle \delta\sigma^4 \rangle - 3 \langle \delta\sigma^2 \rangle) - 12T [(a_1^1)^2 a_2^2 + 2a_1^1 a_2^1 a_2^1] \langle \delta\sigma^2 \rangle^2$$

$$+ 24 [(a_1^1)^3 a_3^1 + 2(a_1^1)^2 (a_2^2)^2] \langle \delta\sigma^2 \rangle^3 + 24(a_1^1)^3 a_2^1 \langle \delta\sigma^2 \rangle \langle \delta\sigma^3 \rangle$$



$$a_k^n = \frac{V}{n!} \frac{\partial^{k+n} \Omega}{\partial \mu^k \partial \sigma^n}$$

Tree level contribution

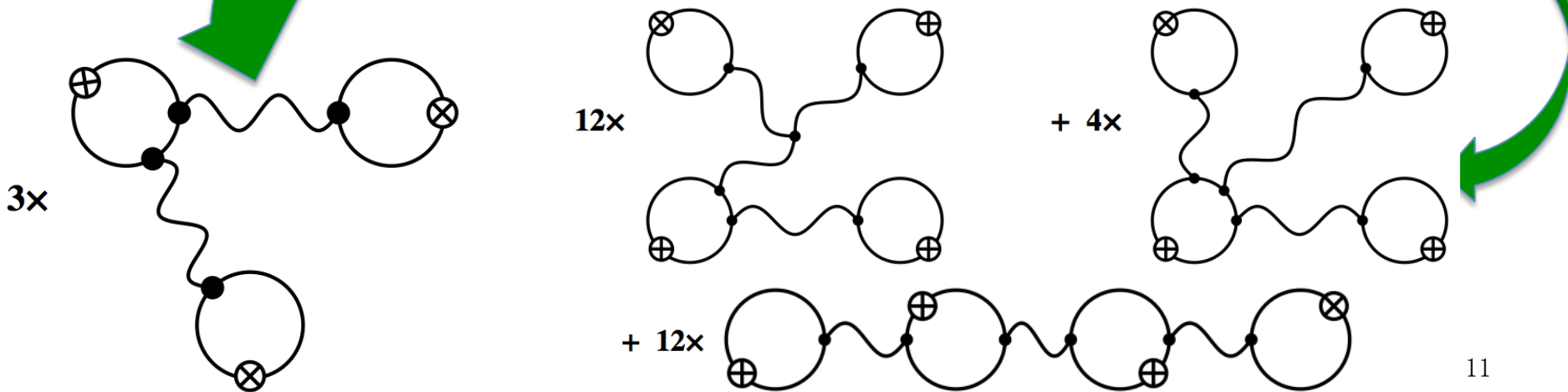
$$T^2 \frac{d^2}{d\mu^2} \log Z = -T a_2^0 + (a_1^1)^2 \langle \delta\sigma^2 \rangle$$

$$T^3 \frac{d^3}{d\mu^3} \log Z = -T^2 a_3^0 + 3T a_1^1 a_2^1 \langle \delta\sigma^2 \rangle - (a_1^1)^3 \langle \delta\sigma^3 \rangle - 6(a_1^1)^2 a_2^2 \langle \delta\sigma^2 \rangle^2$$

$$T^4 \frac{d^4}{d\mu^4} \log Z = -T^3 a_4^0 + 3T^2 (a_2^2)^2 \langle \delta\sigma^2 \rangle + 4T^2 a_1^1 a_3^1 \langle \delta\sigma^2 \rangle - 6T (a_1^1)^2 a_2^2 \langle \delta\sigma^3 \rangle$$

$$+ (a_1^1)^4 (\langle \delta\sigma^4 \rangle - 3 \langle \delta\sigma^2 \rangle) - 12T [(a_1^1)^2 a_2^2 + 2a_1^1 a_2^2 a_1^1] \langle \delta\sigma^2 \rangle^2$$

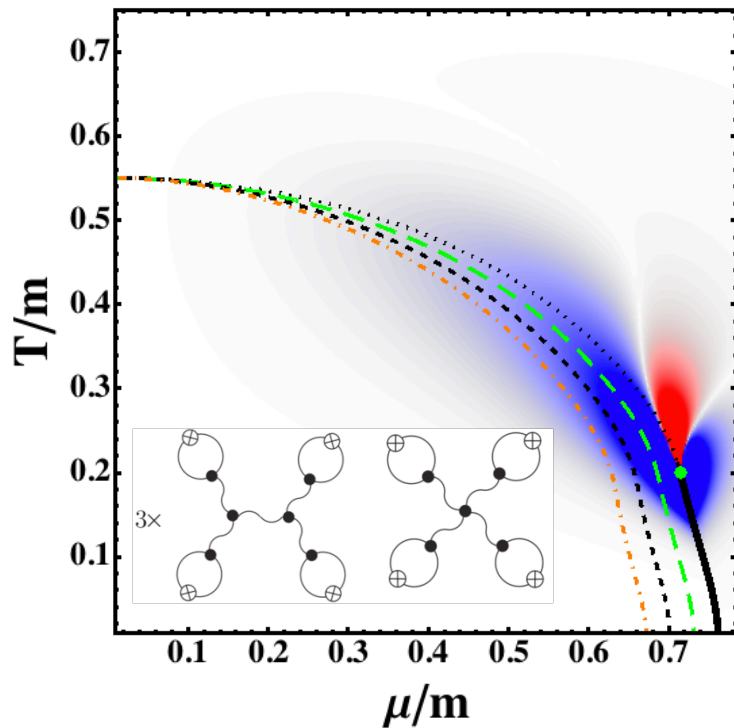
$$+ 24 [(a_1^1)^3 a_3^1 + 2(a_1^1)^2 (a_2^2)^2] \langle \delta\sigma^2 \rangle^3 + 24(a_1^1)^3 a_2^2 \langle \delta\sigma^2 \rangle \langle \delta\sigma^3 \rangle$$



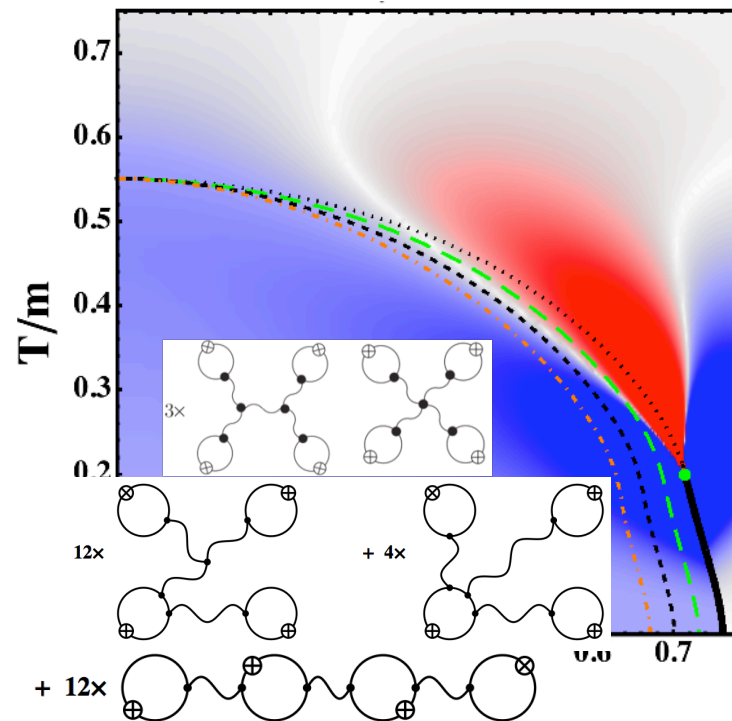
Ratio of the number susceptibilities

$$\kappa_4 = \langle \sigma_V^4 \rangle_c = 6VT^3 [2(\lambda_3 \xi)^2 - \lambda_4] \xi^8$$

$$m_2 = \frac{T^4 \frac{d^4}{d\mu^4} \log Z}{T^2 \frac{d^2}{d\mu^2} \log Z}$$

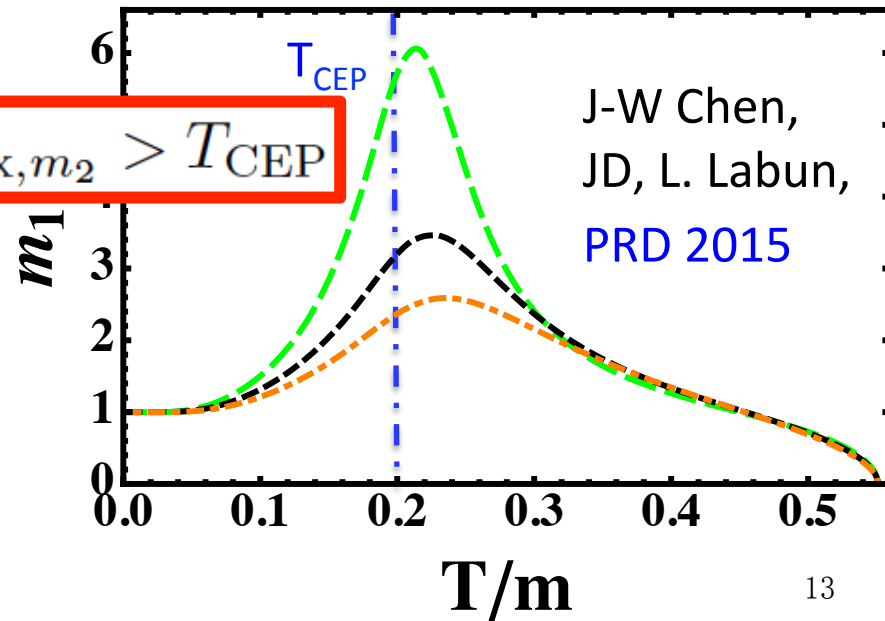
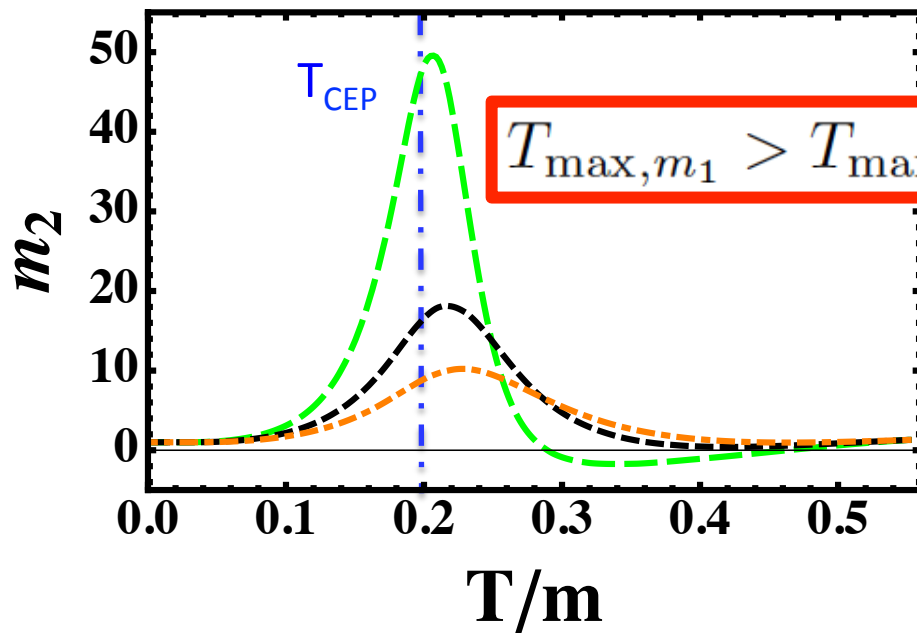
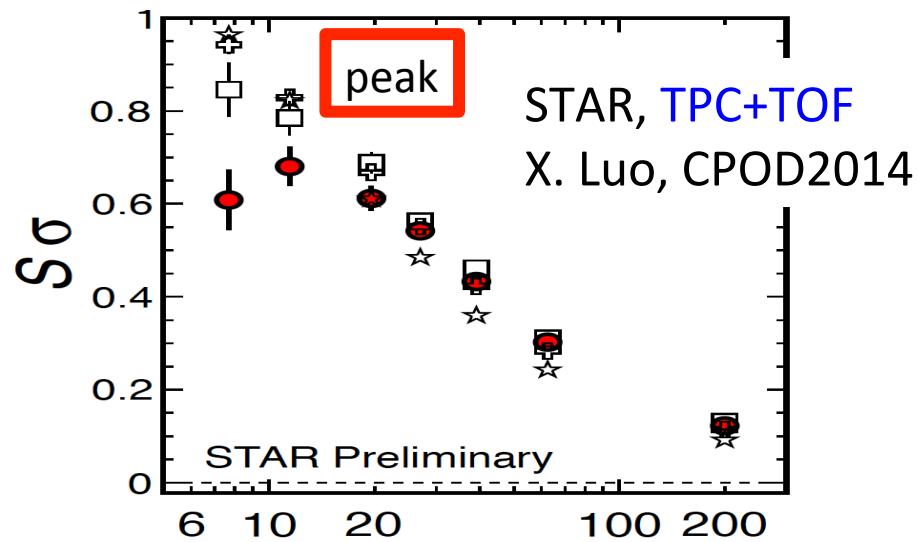
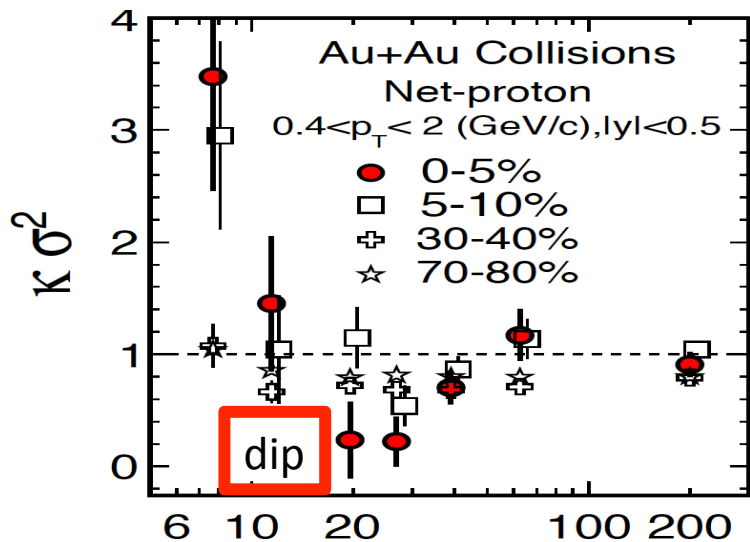


Kurtosis from order parameter fluctuation



There is a large region of negative m_2 , beginning at the critical point and opening up into the crossover region. The negative m_2 region overlaps with the “hadronic” phase near the critical point → non-monotonic feature, sign change!

Comparing with STAR new data



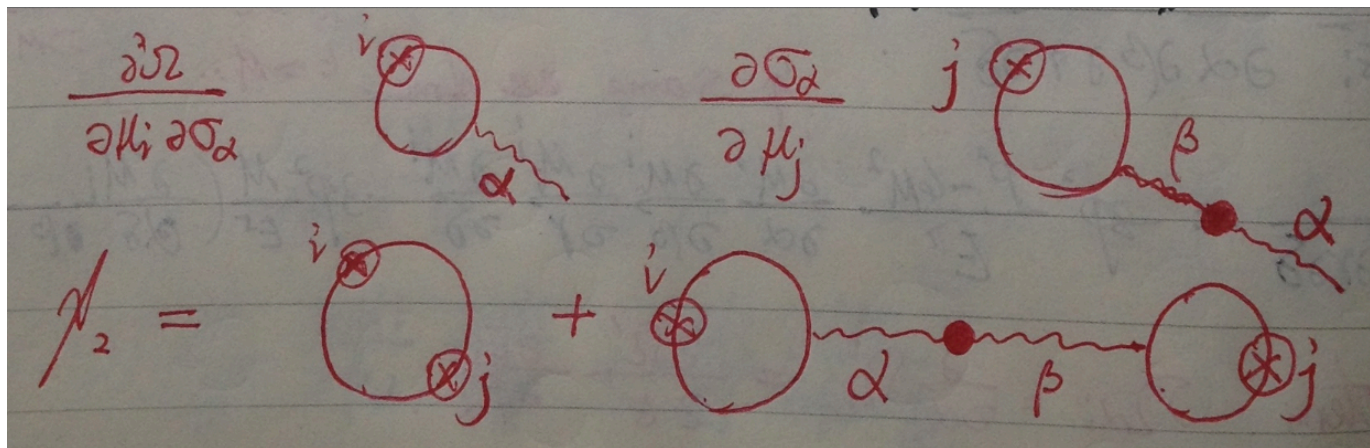
Further study with 3f-NJL model

Effective potential:
Flavor coupled:

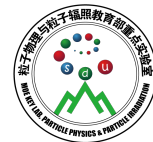
$$\Omega(T, \mu_u, \mu_d, \mu_s) = 2G (\sigma_u^2 + \sigma_d^2 + \sigma_s^2) - 4K\sigma_u\sigma_d\sigma_s + \sum_{f=u,d,s} \Omega_f(T, \mu_f; m_f),$$

$$\Omega_f(T, \mu_f; m_f) = -2N_c \int \frac{d^3p}{(2\pi)^3} \left[E_f \Theta(\Lambda^2 - \vec{p}^2) + T \ln \left[1 + e^{-(E_f - \mu_f)/T} \right] + T \ln \left[1 + e^{-(E_f + \mu_f)/T} \right] \right].$$

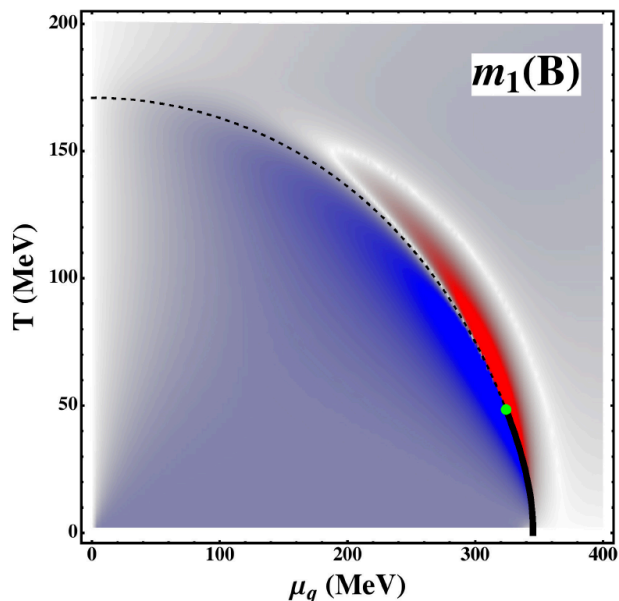
$$E_f = \sqrt{m_f^2 + p^2}, \quad m_f = m_f^0 - 4G\sigma_f + 2K\sigma_{f'}\sigma_{f''}, \quad f \neq f' \neq f'' \in \{u, d, s\}$$



$$\chi_2^{ij} = \left. \frac{\partial^2 \Omega}{\partial \mu_i \partial \mu_j} \right|_{\vec{\sigma}_0} - \sum_{\alpha} \left. \frac{\partial^2 \Omega}{\partial \mu_i \partial \sigma_{\alpha}} \right|_{\vec{\sigma}_0} \left[\left. \frac{\partial^2 \Omega}{\partial \sigma_{\beta} \partial \sigma_{\alpha}} \right|_{\vec{\sigma}_0} \right]^{-1} \left. \frac{\partial^2 \Omega}{\partial \sigma_{\beta} \partial \mu_j} \right|_{\vec{\sigma}_0}$$



Susceptibilities with 3f-NJL model



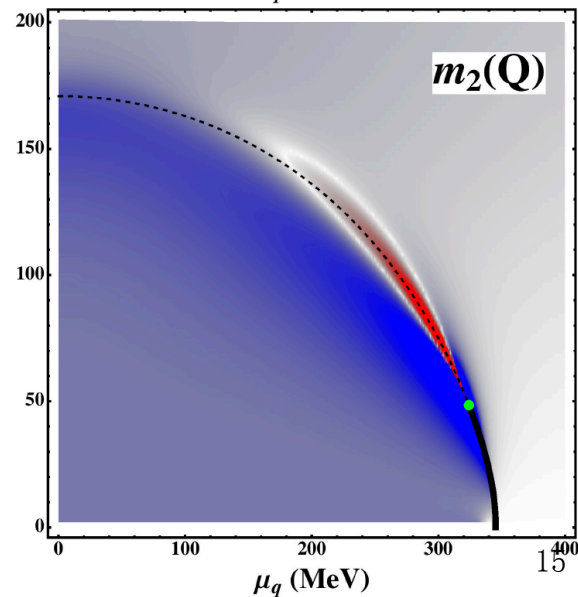
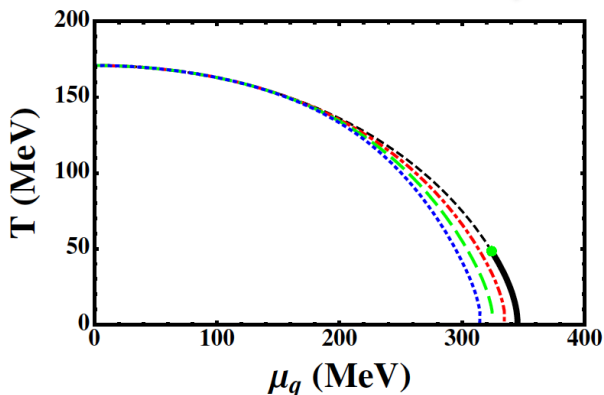
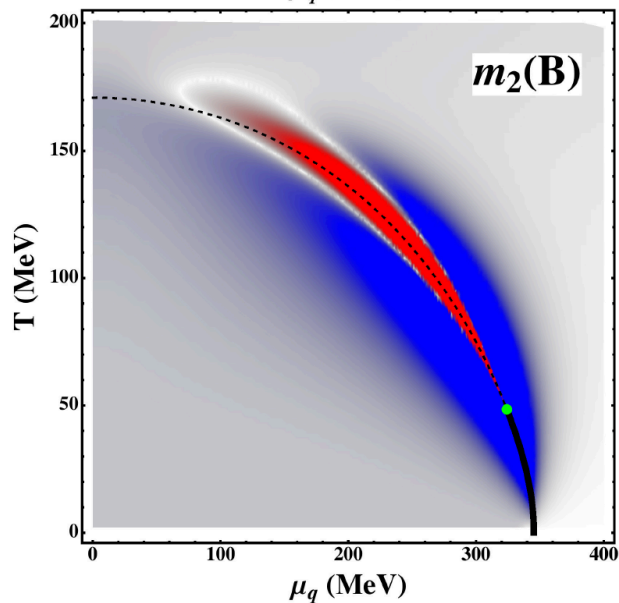
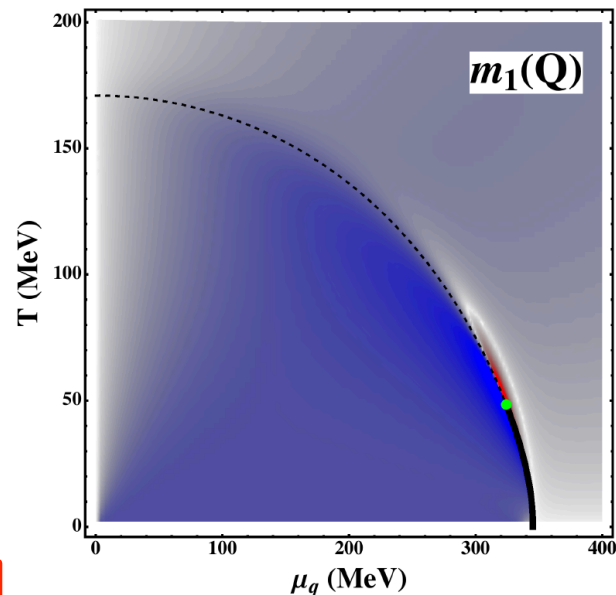
Net Baryon

$$N_B = \frac{1}{3}(N_u + N_d + N_s)$$

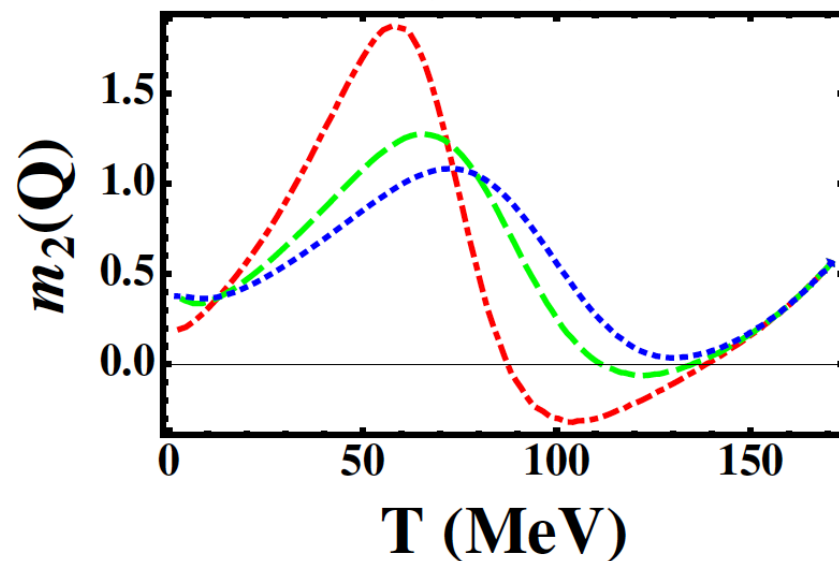
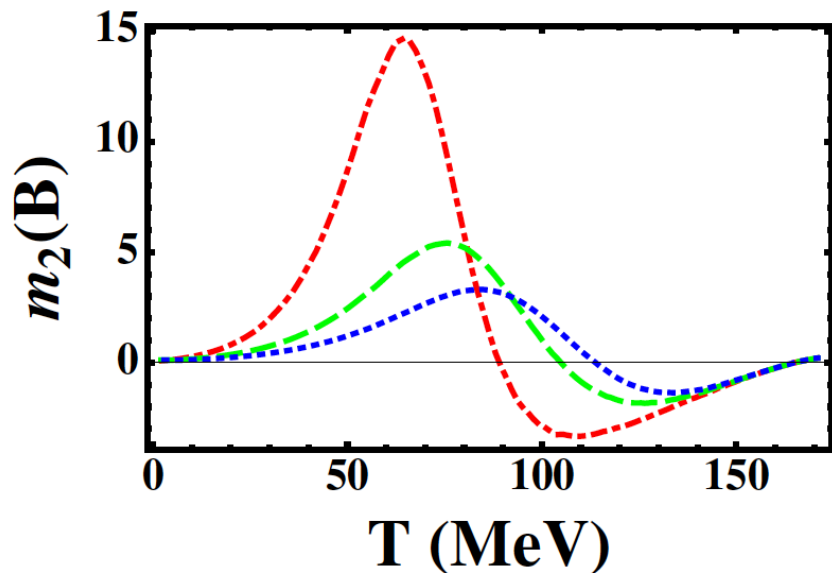
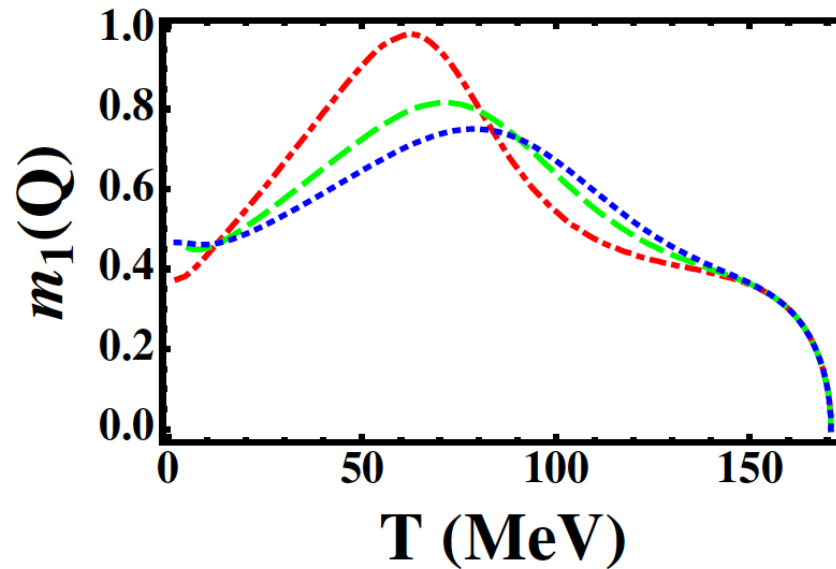
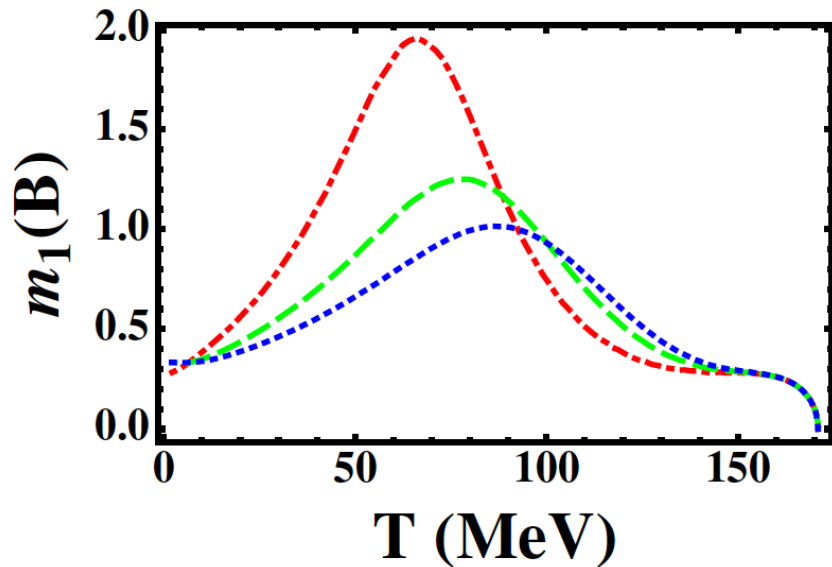


Net Charge

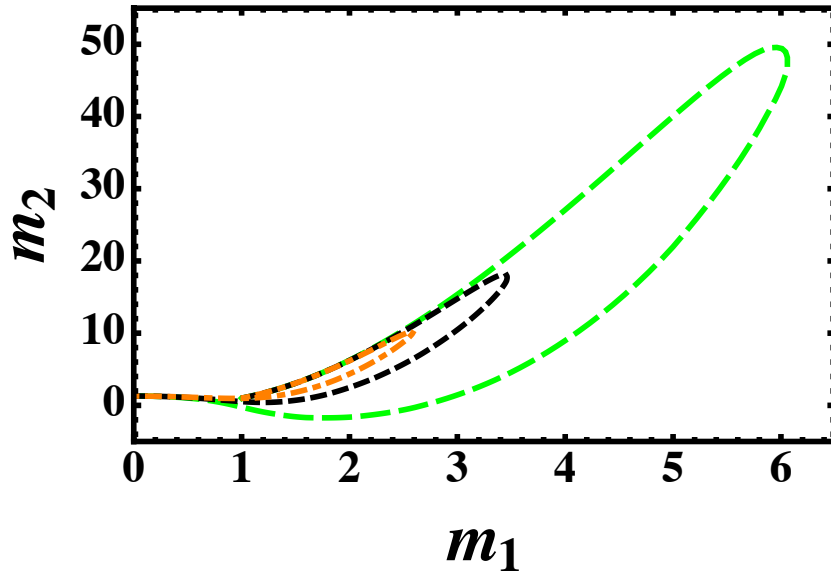
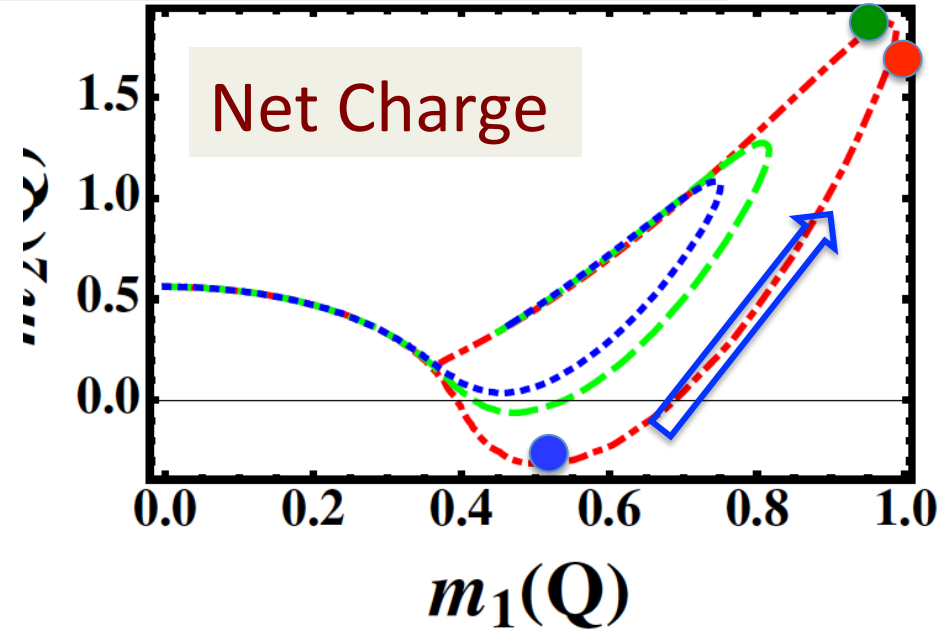
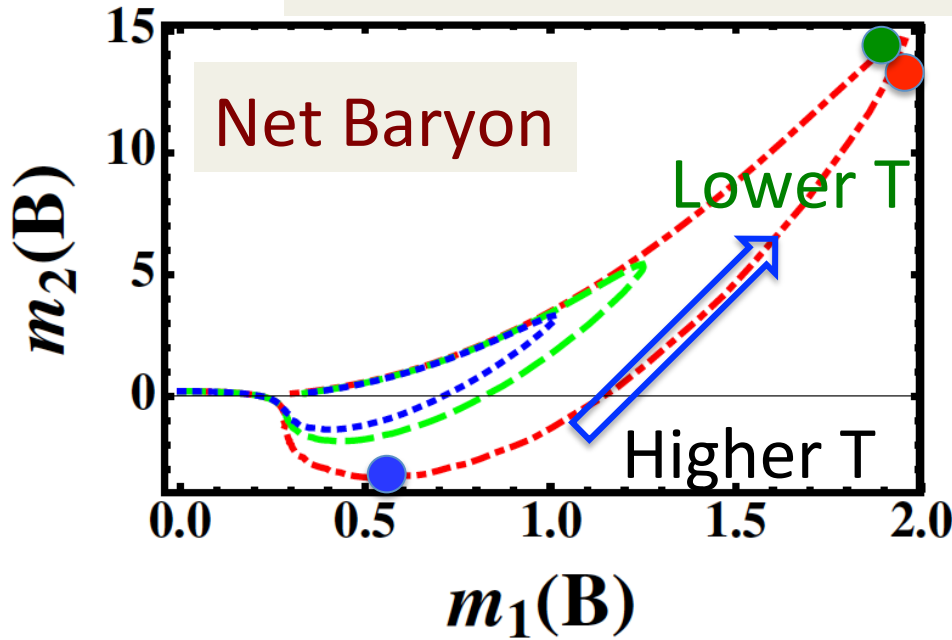
$$N_Q = \frac{1}{3}(2N_u - N_d - N_s)$$



Along hypothetical Freeze-out lines



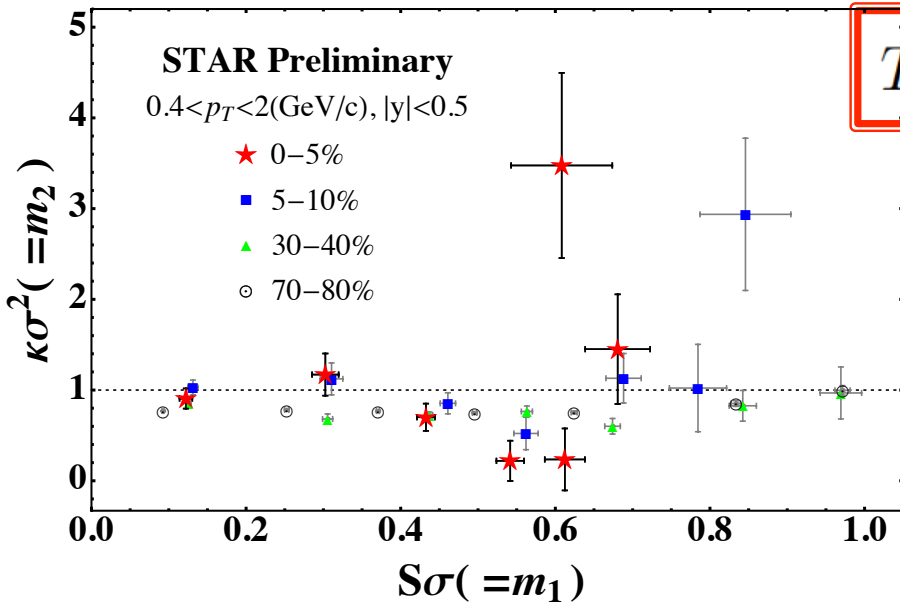
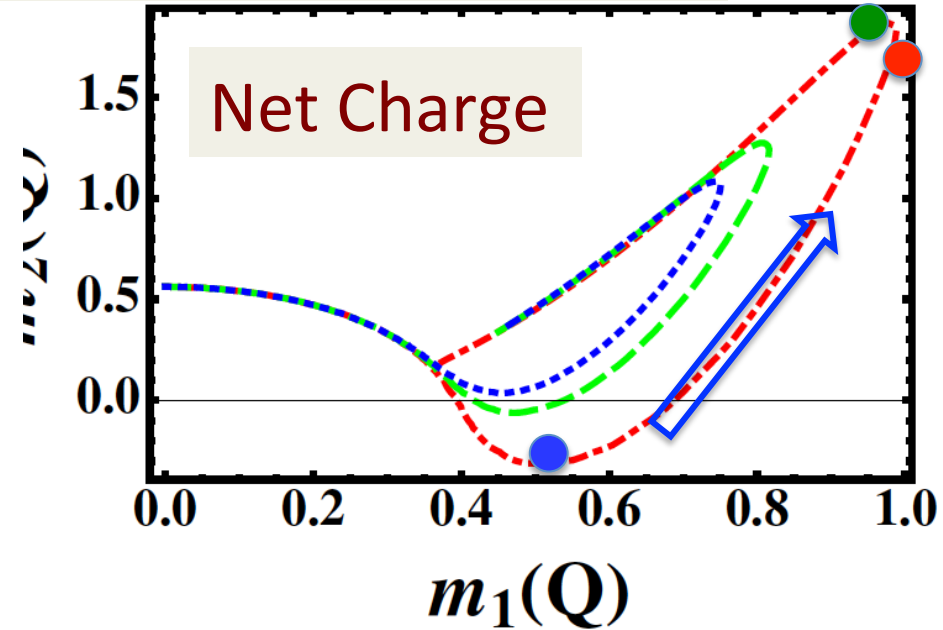
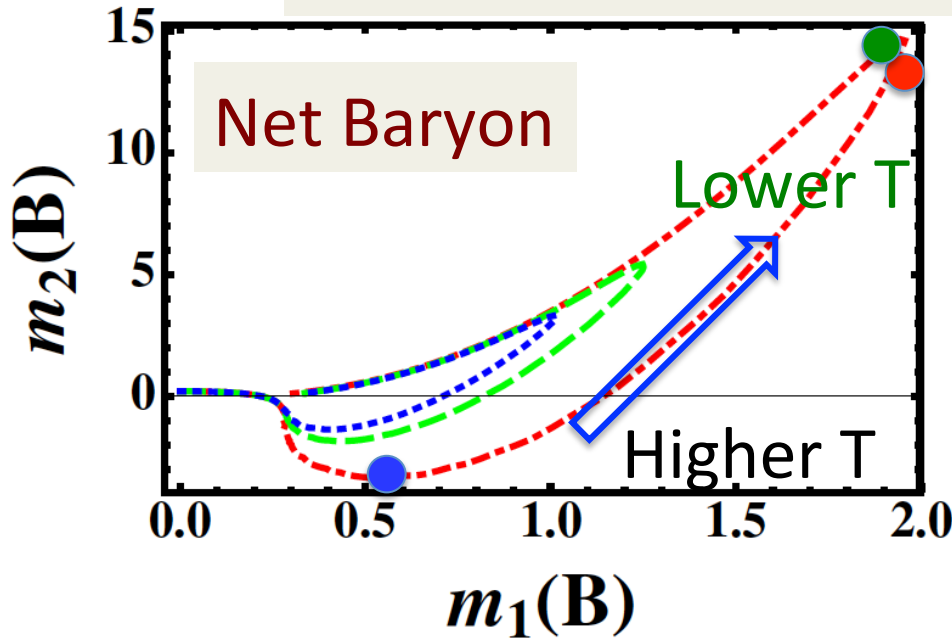
Combination of m_1 and m_2 , common?



$$T_{\min, m_2} > T_{\max, m_1} > T_{\max, m_2} > T_{\text{CEP}}$$

- also seen with Ising model
- robust features of CP
- survive after non-thermal effects

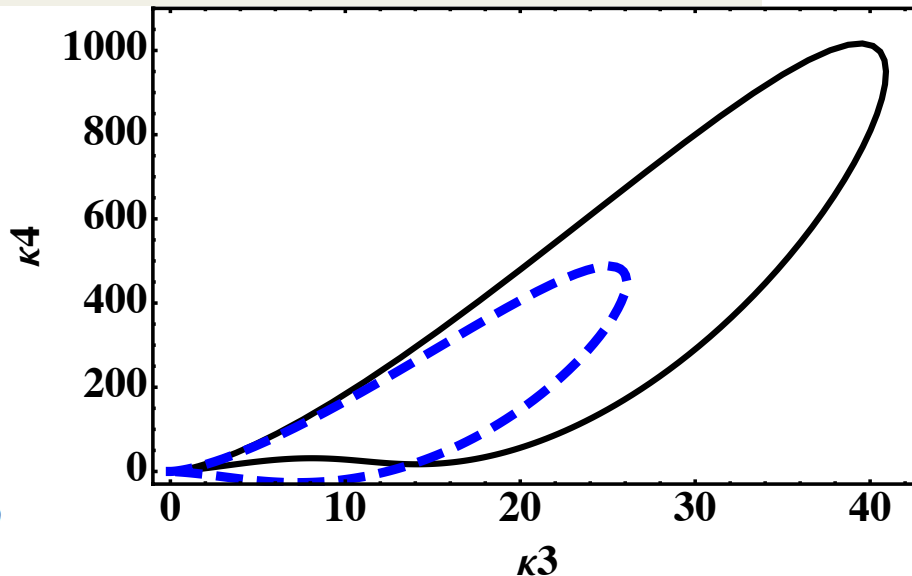
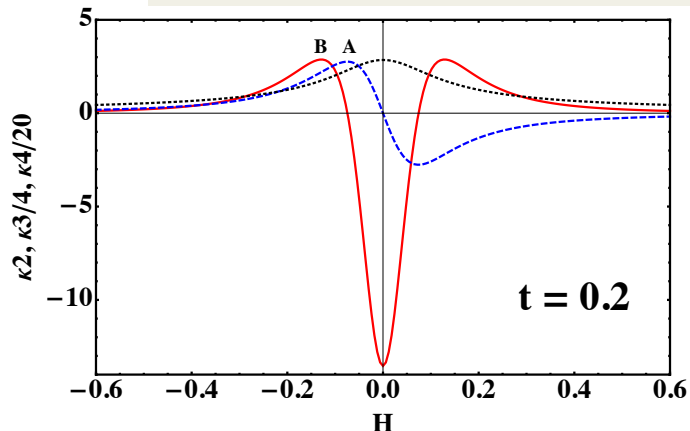
Combination of m_1 and m_2 , common?



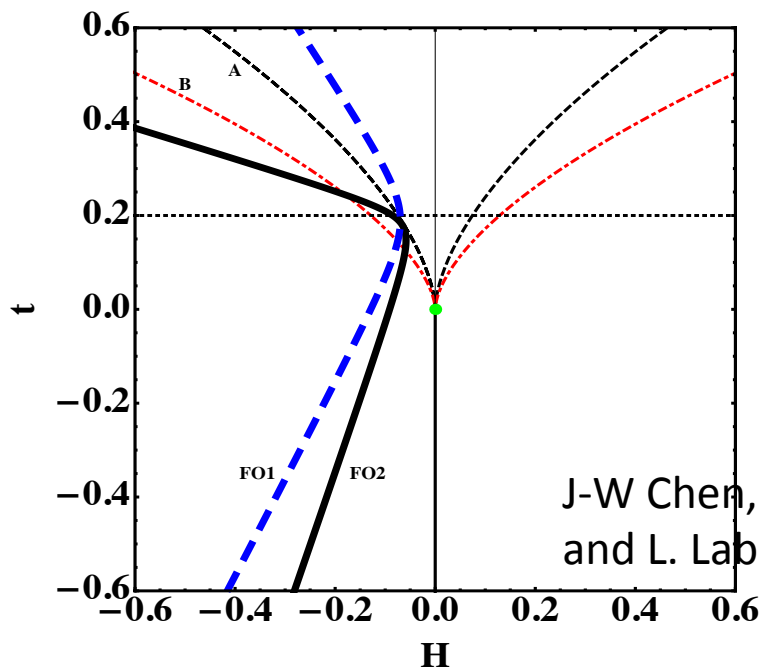
$$T_{\min, m_2} > T_{\max, m_1} > T_{\max, m_2} > T_{\text{CEP}}$$

- also seen with Ising model
- robust features of CP
- survive after non-thermal effects

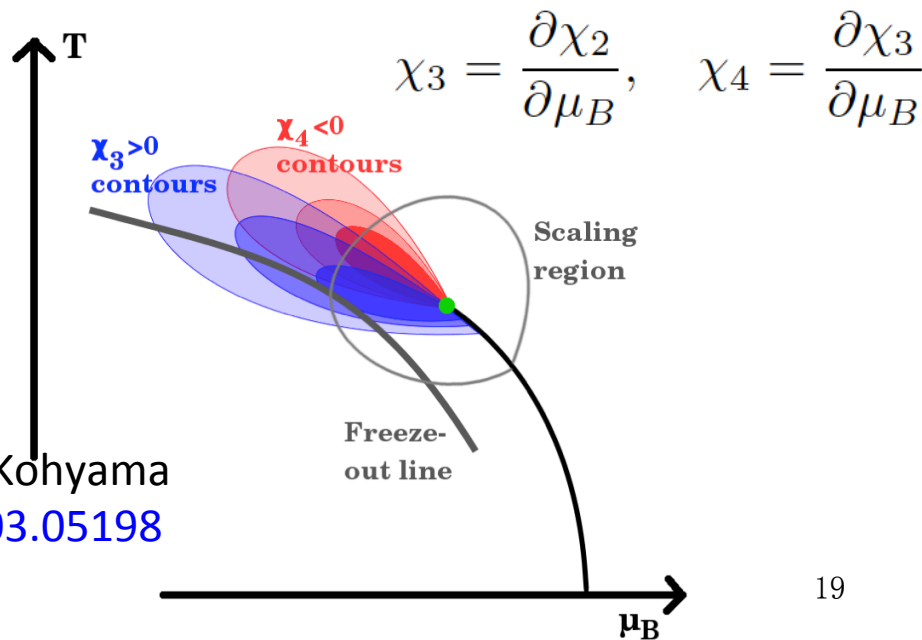
Reasons for T ordering



$$\kappa_2 \equiv \frac{\partial M}{\partial H}, \quad \kappa_3 = \frac{\partial \kappa_2}{\partial H}, \quad \kappa_4 = \frac{\partial \kappa_3}{\partial H},$$

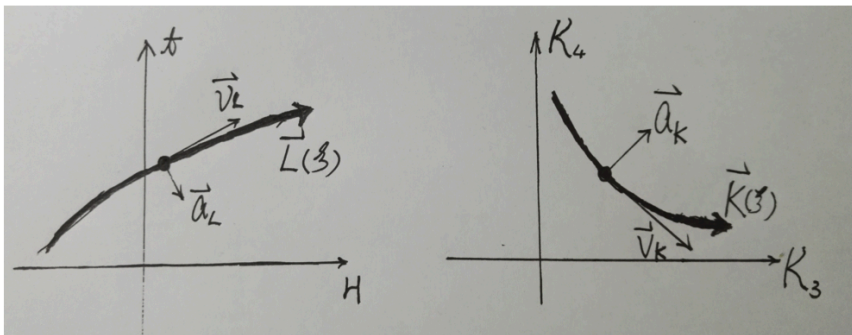


J-W Chen, JD, H. Kohyama
and L. Labun, [1603.05198](#)



Reasons for T ordering

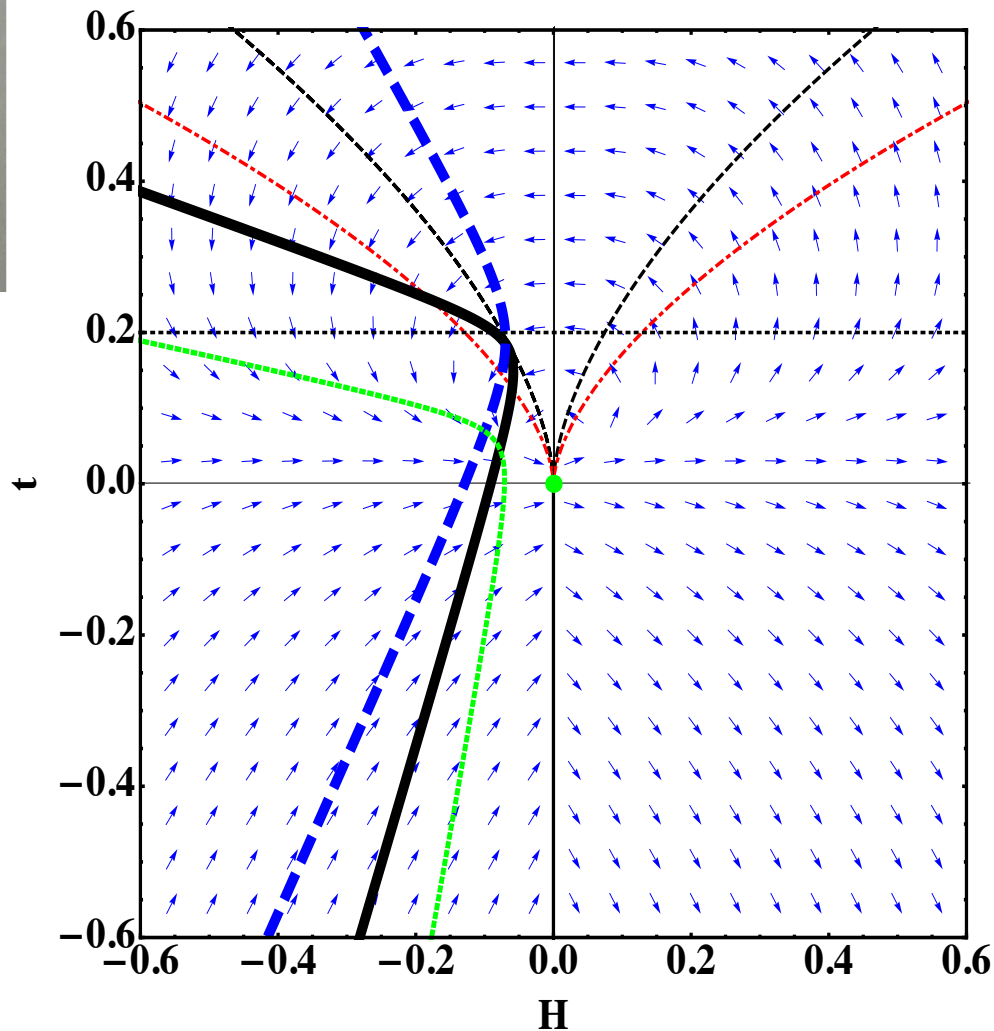
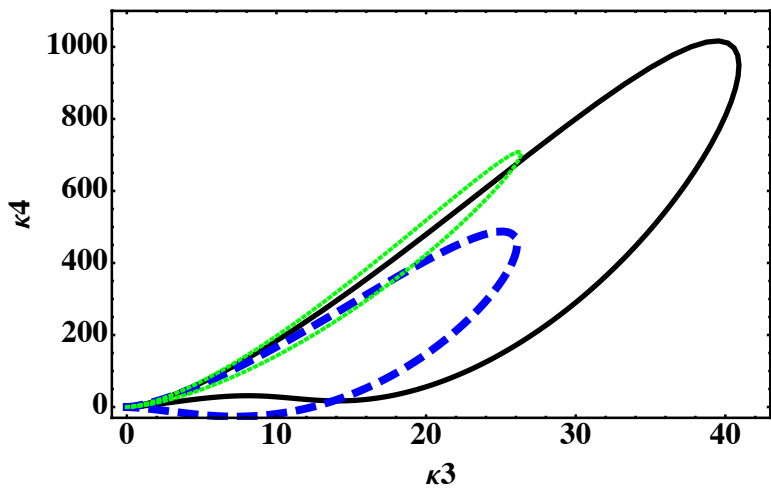
$$(\vec{v}_K \times \vec{a}_K)_z = (\vec{\nabla}_{\kappa_3} \cdot \vec{v}_L)(\vec{v}_L \cdot \square \kappa_4 \cdot \vec{v}_L) - (\vec{\nabla}_{\kappa_4} \cdot \vec{v}_L)(\vec{v}_L \cdot \square \kappa_3 \cdot \vec{v}_L) + (\vec{\nabla}_{\kappa_3} \times \vec{\nabla}_{\kappa_4}) \cdot (\vec{v}_L \times \vec{a}_L)$$



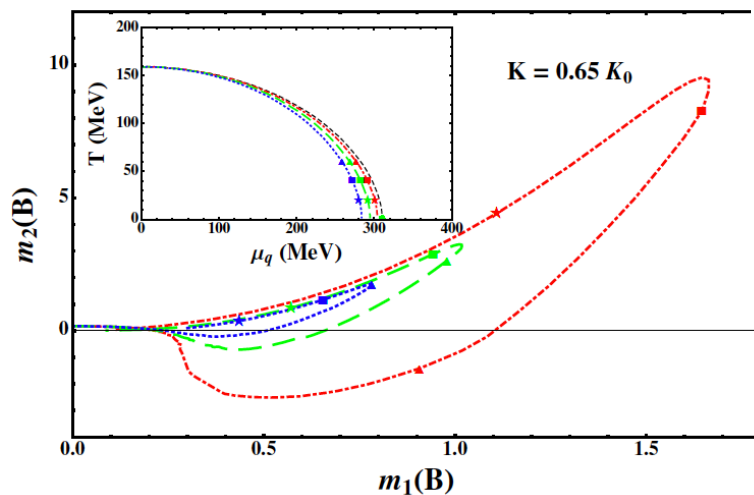
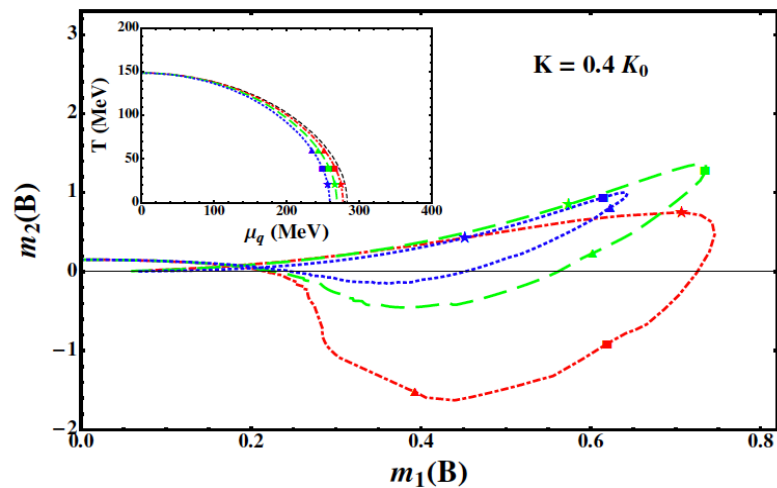
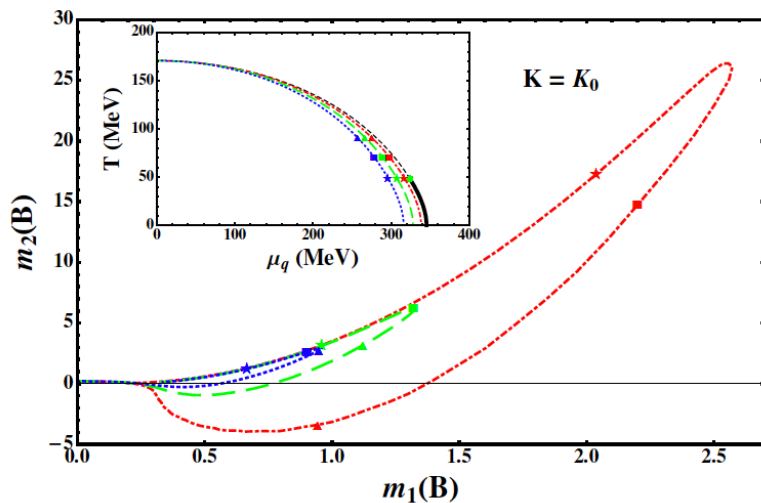
$$\vec{L}(\xi) = \vec{L}_0 + \vec{v}_L \Delta \xi + \frac{1}{2} \vec{a}_L \Delta \xi^2 + \dots,$$

$$\vec{K}(\xi) = \vec{K}_0 + \vec{v}_K \Delta \xi + \frac{1}{2} \vec{a}_K \Delta \xi^2 + \dots,$$

$$\vec{\nabla}_{\kappa_i} = \left(\frac{\partial \kappa_i}{\partial H}, \frac{\partial \kappa_i}{\partial t}, 0 \right), \square \kappa_i = \begin{pmatrix} \frac{\partial^2 \kappa_i}{\partial H^2} & \frac{\partial^2 \kappa_i}{\partial H \partial t} & 0 \\ \frac{\partial^2 \kappa_i}{\partial H \partial t} & \frac{\partial^2 \kappa_i}{\partial t^2} & 0 \\ 0 & 0 & 0 \end{pmatrix}$$

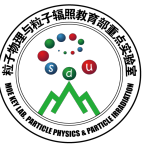


CP and the loops



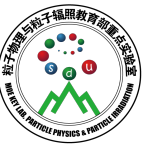
$$T_{\min, m_2} > T_{\max, m_1} > T_{\max, m_2} > T_{\text{CEP}}$$

- CP \rightarrow Banana \rightarrow T ordering
- $m_2 \gg m_1 \geq 1 \rightarrow$ FO near CP
- Serve as a first check for CP
- BES-II, $\sqrt{s_{\text{NN}}} < 20 \text{ GeV}$, can answer



Summary

1. QCD phase diagram with **CP** are explored. Higher order susceptibilities and relations between observables are crucial.
2. Sign change of m_2 , and peak in m_1 indicate non-monotonic behaviors. **The banana shape of m_2 vs. m_1** , and ordering $T_{\min, m_2} > T_{\max, m_1} > T_{\max, m_2} > T_{\text{CEP}}$ help to indicate the location of CP.
3. Data comparison shows **QCD criticality**. **CP** is needed to explain the data. BES-II will answer ...



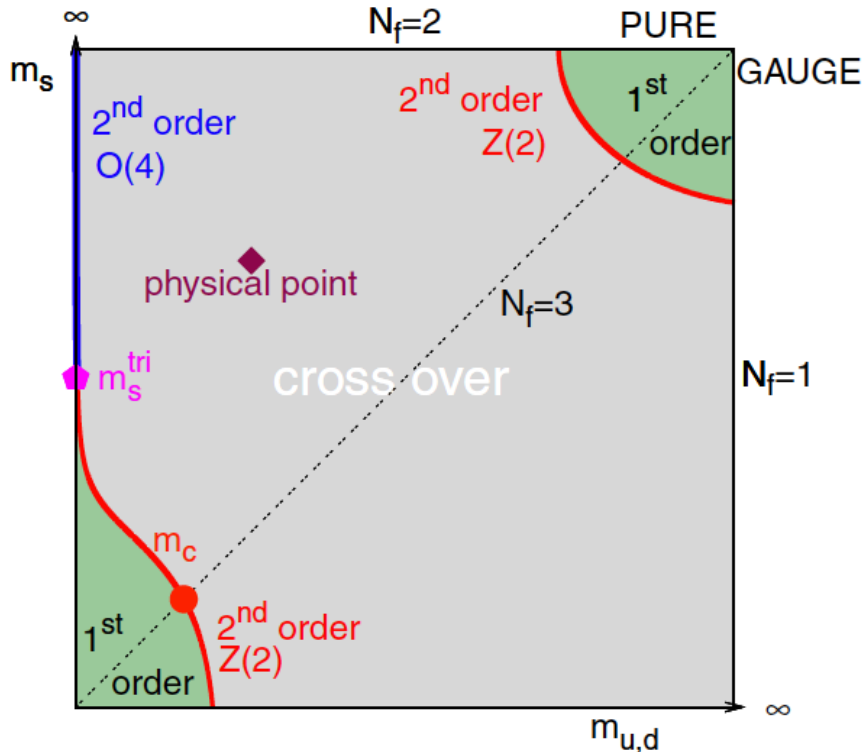
Summary

1. QCD phase diagram with **CP** are explored. Higher order susceptibilities and relations between observables are crucial.
2. Sign change of m_2 , and peak in m_1 indicate non-monotonic behaviors. The banana shape of m_2 vs. m_1 , and ordering $T_{\min, m_2} > T_{\max, m_1} > T_{\max, m_2} > T_{\text{CEP}}$ help to indicate the location of CP.
3. Data comparison shows **QCD criticality**. **CP** is needed to explain the data. BES-II will answer ...

Thanks

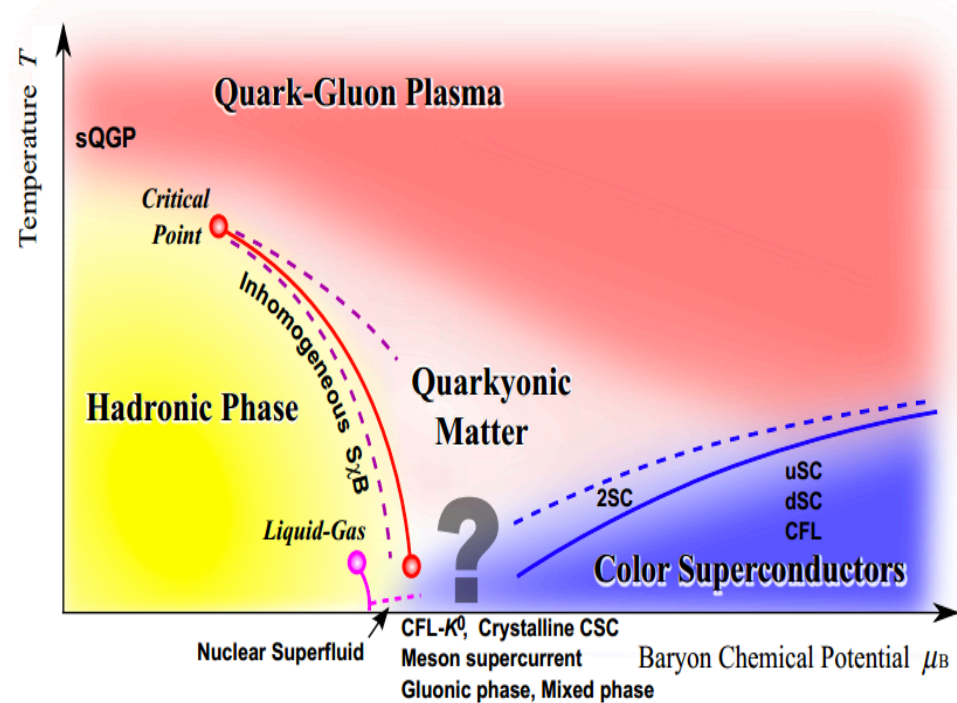
Back up

Phase transition and CP within QCD



F. R. Brown, et al. [PRL 1990](#)
[Full lattice QCD simulation](#)

Because the relevant symmetry is explicitly broken by quark mass, symmetry arguments no longer imply the existence of a finite temperature phase transition.

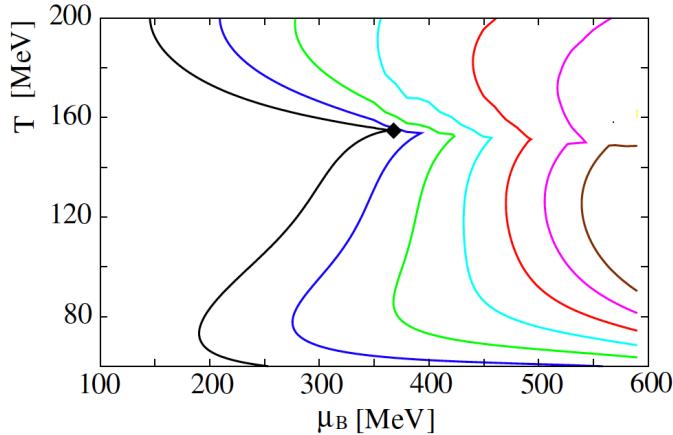


K. Fukushima and T. Hatsuda
[Rep. Prog. Phys. 2010](#)

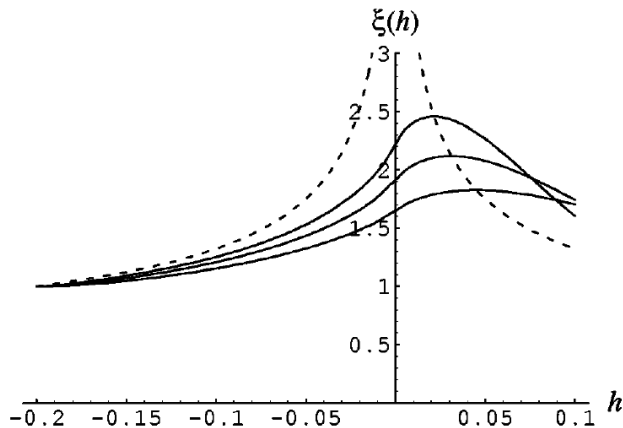
Even no reliable information from the first-principle LQCD calculation, effective chiral models suggest a first order chiral phase transition in the large density region.

CEP in HIC

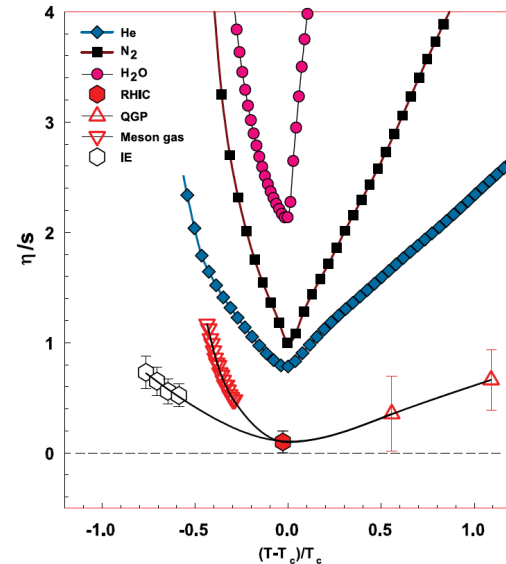
Crucial in diagram, test QCD in **non-perturbative** region



Attractor for thermodynamic trajectories in HIC. C. Nonaka and M. Asakawa, [PRC 2005](#)

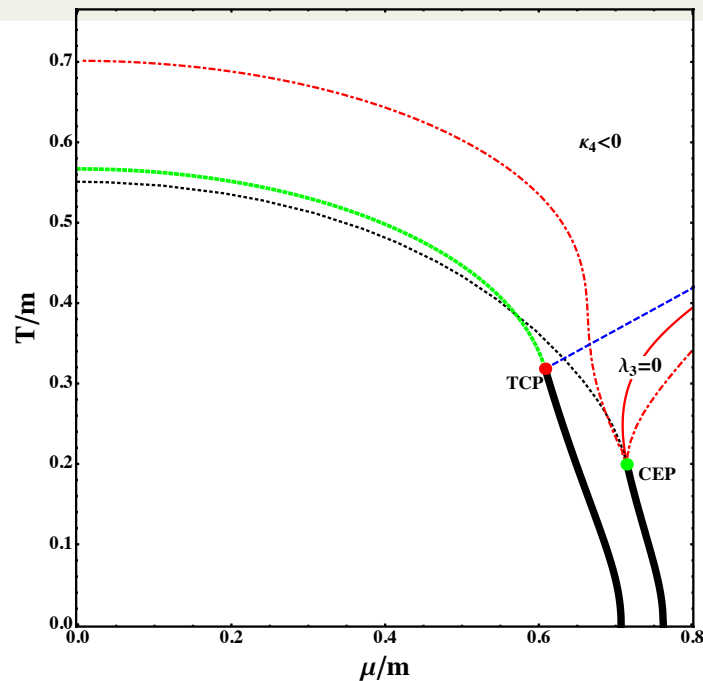
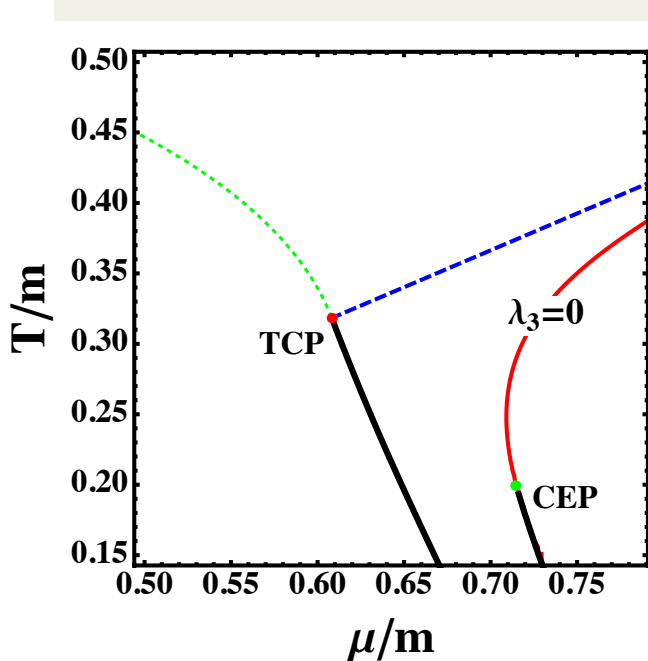


Slowing out of equilibrium near CEP
B. Berdnikov and K. Rajagopal, [PRD 2000](#)



Most difficult for momentum transport near CEP
Roy A. Lacey, et al. [PRL 2007](#)

Key features with Gross-Neveu model



J-W Chen,
JD, L. Labun,
PRD 2015

$$\kappa_3 = \langle \sigma_0^3 \rangle = \frac{2\lambda_3 T}{V} \xi^6; \quad \kappa_4 = \langle \sigma_V^4 \rangle_c = 6VT^3 [2(\lambda_3 \xi)^2 - \lambda_4] \xi^8;$$

The line $\lambda_3 = 0$ does **NOT** lead the crossover line!
but separates the positive and negative region of skewness,
guides the negative region of kurtosis of the sigma field.

Time evolution of cumulants (memory)

Critical slowing down

$$\frac{dP}{d\tau} = F[P]$$

\Downarrow

$$\frac{d\kappa_n}{d\tau} = L[\kappa_n, \kappa_{n-1}, \dots]$$

